Evaluation of the Long-term Cumulative UVA Facial Exposure of Queensland School Teachers derived for an Extended Period from the OMI Satellite Irradiance

Mustapha A. A Jebar[1,3], Nathan J. Downs[1,2], Alfio V. Parisi[1,2,*] and Joanna Turner[1]

[1]University of Southern Queensland, Faculty of Health, Engineering and Sciences, Toowoomba, Australia

[2]Centre for Applied Climate Sciences, University of Southern Queensland, Toowoomba, Australia

[3]Physics Department, Faculty of Sciences, University of Thi Qar, Iraq

* corresponding author email: parisi@usq.edu.au (Alfio V. Parisi)

ABSTRACT

This research presents a novel methodology for deriving the total daily broadband solar UVA (320-400 nm) received by school teachers during their working day from Ozone Monitoring Instrument (OMI) satellite solar noon UVA irradiance measurements for a Queensland sub-tropical site (27.5ºS, 152ºE). Daily UVA exposures are weighted to the anatomical human cheek (anterior infra-orbital region) for teachers wearing, and not wearing broad-brimmed hats. The method utilizes the OMI UVA irradiance data collected daily at high temporal resolution over 2005 to 2016 to derive the total daily UVA exposure to a horizontal plane. These horizontal plane exposures are scaled by factors to take into account the timing of outdoor activity. The relationship between exposures to a horizontal plane and those to a vertical plane and the protection provided by a broad-brimmed hat were assessed to evaluate the total daily UVA exposures to the cheek for classroom and physical education teaching staff expected to be outside at different periods of the day. The developed method enables the total daily UVA exposure to specific anatomical sites to be evaluated from the satellite solar noon irradiance at locations that do not have access to surface-based instrumentation capable of recording in the solar UVA waveband.

INTRODUCTION

Surface-based UV radiometers are used to measure the UVA and UVB irradiance but do not provide sufficient coverage to monitor the majority of the earth's surface, especially over the oceans (1). Interest in terrestrial (and marine) UV radiation reaching the earth's surface over the past few decades has created increasing demand for satellite-based instrumentation. Approaches that depend on satellite data are suitable alternatives to surface-based instrumentation because satellites have the capability to determine important parameters over a wide area and provide reasonable estimates of the UV irradiance where local surface instrumentation is not available (2, 3). Satellite based instrumentation has been employed for the provision of global coverage on a time repetitive basis of the atmospheric ozone, aerosols, UVA and UVB at specific wavelengths. There are several satellite platforms that monitor UV radiation that continue to provide a growing body of data enabling remote investigation of local UV climatology in the mid- to long-term. These have provided high spatial and temporal resolution datasets from the late 20th century to the present day, and include: TOMS, GOME, MODIS and OMI satellite platforms (4).

Data retrieved from satellites is often limited between one and several local passes per day, making the full construction of the diurnal variation in solar UV irradiance challenging, while at the same time there is a need for long-term estimates in UV climatology. Langston (5) recently derived annual erythema weighted exposure integrals from single pass satellite noon-time UVB irradiance estimates. Similarly, for cloud-free conditions a technique based on a Gaussian curve has been employed to evaluate the daily erythemal UV exposure from the maximum UV index (6) however, there is no readily applicable approach to calculate the daily UVA exposures from a single value. This research will develop a new methodology to calculate the daily UVA exposures from the UVA irradiance at solar noon. The developed technique will be applied to evaluate the occupational solar UVA exposures over an extended period to a specific anatomical site of both physical education, and classroom teaching staff groups with different hat wearing practices.

MATERIALS AND METHODS

The evaluation of the daily ambient UVA exposure was derived by numerical integration of the expected daily irradiance distribution for a Southern Queensland site

(27.5ºS, 152ºE). The normalized daily distribution of the UVA exposure in five-minute intervals were evaluated using ground-based UVA data for the period 2005 to 2016 to allow determination of a scaling factor to relate local solar noon values to the total daily UVA exposure. The daily UVA exposures were then modeled with the use of this scaling factor multiplied by the maximum daily broadband UVA irradiance derived remotely from the OMI satellite for solar noon. The diurnal UVA exposure was then expressed relative to an upright cylindrical plane representing the expected facial site exposure of an upright human model. This exposure was employed to calculate the occupational UVA exposure over a period of 12 years to the cheek (anterior infra-orbital facial region) by weighting with the expected outdoor activity index, and facial site protection factors for both physical education and classroom teaching staff. The physical education and classroom teachers were employed as outdoor activity data were available for this occupational group. Cumulative occupational UVA exposure totals derived from the entire 2005 to 2016 monitoring period are presented for both teaching classifications and compared between staff who may or may not choose to wear a broad-brimmed hat daily over the entire 12-year interval.

Diurnal Course of UVA Irradiance

The total daily radiant UV exposure for a particular waveband, H_{Day} (J/m^2) is the integral of the changing daily solar UV irradiance, E (W/m^2) measured from sunrise to sunset. H_{Day} may be determined for the length of a solar day [normalized as t = 0 to 1] according to Equation 1:

$$H_{Day} = \int_{t=0}^{1} E(t)dt \qquad (1)$$

where E under cloud free conditions is dependent on the diurnal variation in air mass and is a function of local solar zenith angle (SZA), increasing from sunrise, reaching a maximum on cloud free days at solar noon, and decreasing steadily to sunset. As the radiant UVA exposure is measured between the wavelength range, λ_{min} = 320 to λ_{max} = 400 nm (7), the diurnal variation of E is largely independent of atmospheric absorption by ozone, a significant regulator of terrestrial UVB irradiance which falls to negligible attenuation in the UVA for wavelengths above 330 nm (8). Thus, the

variation of *E* under cloud-free conditions follows a predictable daily distribution. Figure 1 shows the ground-based measured distribution in UVA and erythemal UV exposures over five-minute periods divided by the respective maximum daily value. This time period was used as the data from the ground-based radiometers were recorded every five minutes. The UVA exposure over a five-minute period was plotted at each hour to show the change over the day. The data were measured over 186 cloud free days between October 2004 and December 2016 at the University of Southern Queensland solar radiation monitoring site (27.5^{o}S, 152^{o}E). The cloud-free measurements were made using two independent radiometers, one measuring the UVA waveband (model 501 UVA, Solar Light Co., PA. USA) and one measuring the erythemal weighted UV waveband (model 501, Solar Light Co., PA, USA). The data from the UVA waveband radiometer were calibrated over this period to a scanning spectroradiometer (model DTM300, Bentham Instruments, Reading, UK) with irradiance calibration traceable to the National Physical Laboratory, UK standard and wavelength calibrated against the UV spectral lines of a mercury lamp.

>Figure 1<

Radiant UV exposure curves were included in the figure for all days in the 12-year measurement period only if the day was determined to be cloud-free. Cloud free days were those in which no cloud was detected in the daily recording period (from local sunrise to sunset). From Fig. 1, variations observed in the measured peak UV exposure and the length of the daily exposure interval are caused by the seasonal influence in local sunrise and sunset times and noon SZA, where the longest days and minimum SZA (maximum UV) occur in late December, near the Southern Hemisphere summer solstice and the perihelion passage of the Earth's annual orbit, occurring in early January. The data in Fig. 1 shows that the shape of the curves during the day is different for the UVA waveband compared to the erythemal UV waveband.

Each of the data-series plotted for both the UVA and the erythemal UV wavebands in Fig. 1 was normalized with respect to the peak UV and with respect to the day length (Fig. 2) from sunrise to sunset. The normalization of both axes for each of 186 cloud free exposure days results in the production of a nominal range and domain function [0

to 1] on both axes, where the normalized curves in Fig. 2 were found by application of Equations 2 and 3:

$$N(x) = \frac{Hour(x)}{Hour_{sunset}(x) - Hour_{sunrise}(x)} \quad (2)$$

$$E(x) = \frac{E_{UV}(x)}{E_{UVmax} - E_{UVmin}} \quad (3)$$

where, $N(x)$ is the normalized day light fraction expressed as a fraction of the measured number of hours, from sunrise and sunset, where x represents time and the day length $(Hour_{sunset}(x) - Hour_{sunrise}(x))$ was determined from the first and last non-zero measurement of E_{UV} for each of the 186 cloud free days in the 12-year measurement period. Similarly, the normalized five-minute radiant exposure, $E(x)$ is expressed as a fraction by calculation of the quotient of $E_{UV}(x)$ at each recorded time of day to the daily range in UV exposure of E_{UVmin} to E_{UVmax}. The reason for doing this is to correct the data for seasonality. As a result, the integral of the normalized cloud-free exposures represents a unit-less nominal integral occupying a one times one grid space in x and y. The resulting normalized erythemal and UVA data which all fall within the thick black curve shows little variation across all 186 UV curves which are spread across all of the seasons when re-plotted in Fig. 2 as the influence of seasonality has been removed through the normalisation of the cloud free data using Equations (2) and (3).

A Gaussian distribution has been used previously (6) to estimate the total erythemally weighted daily UV exposure. From Fig. 2(a), the normalized UVA curves exhibit less tapering near sunrise and sunset then approximated by a Gaussian distribution function. This is a likely consequence of the UVA exposure distribution curve being less sensitive to Rayleigh's criterion for scattering at large solar zenith angle (SZA). This shows that the Gaussian distribution is better suited to evaluating the daily total erythemal UV exposure and is not as suitable for determining the total daily UVA exposure. Consequently, a trapezoidal integral approximation (Equation 4) was used to derive the normalized daily UVA radiant exposure, S according to:

$$S \approx \frac{0.05}{2}(E(0) + E(1) + 2\sum_{i=1}^{n} E(x_i)), \quad (4)$$

where, $E(0)$ and $E(1)$ represent the starting and terminating normalized exposure and $E(x_i)$ represents the normalized UVA exposure at each step in the numerical integral between the $E(0)$ and $E(1)$. The factor of 0.05/2 is common to each of 20 trapeziods used to approximate the nomalised integral in 20 steps in time, x from 0 through 1. $E(x)$ at each step therefore represents the daily normalized UVA irradiance measured in steps ranging from approximately 30 to 40 minutes in length between winter (10 daylight hours) and summer (14 daylight hours) respectively.

>Figure 2<

Daily UVA radiant exposure

The integral of the UVA normalized distributions was utilized to develop an approximation for the predicted daily UVA_{Day} under cloud free conditions (9):

$$UVA_{DAY}[kJ/m^2] = \frac{I \times 3600 \times N \times S}{1000}, \quad (5)$$

where the daily UVA integral expressed in kJ/m^2 is modeled by scaling the maximum noon irradiance, I [W/m^2] measure by OMI satellite expressed in Joules per hour multiplied by the number of daylight hours, $N = (Hour_{sunset}(x) - Hour_{sunrise}(x))$ and the numerical integral, S derived by equation 4. The solar noon UVA irradiance has been evaluated from the OMI satellite spectral irradiance measured at 310 nm, 324 nm and 380 nm (10). The value of S has previously been determined for both cloud free and cloudy days for the cases of the sun obscured and the sun not obscured, enabling the use of equation (5) for the range of cloud conditions encountered (9). These are S = 0.50, 0.45, 0.42 and 0.42 respectively for the sun not obscured categories of 0-2, >2-4, >4-6 and >6-8 octas of cloud cover and S = 0.41, 0.39 and 0.37 respectively for the sun obscured categories of 2-4, >4-6 and >6-8 octas. These values of S are applicable across all of the seasons as the data has been normalized according to Equations (2) and (3). This is illustrated in Fig. 2 where all of the 186 normalized daily curves for the cloud free cases across all of the seasons fall within the thick black curve. The total daily UVA exposures calculated with these values of S from the OMI satellite data were

validated against the daily UVA exposures over 2015 and 2016 measured by the previously mentioned ground-based UVA radiometer at the site of this research (9). The validation provided a mean absolute error (MAE) of 84.2 kJm^{-2} (10%) for the sun not obscured cases and a MAE of 138.4 kJm^{-2} (30%) for the sun obscured cloudy days.

The average of the sun not obscured *S* values of 0.448 was used to take into account the range of cloud conditions encountered. The average was only taken of the sun not obscured cases as these provide the worst-case scenario compared to the sun obscured cases. The constants 3600, and *N* account for the number of seconds in the day where *N* represents the number of hours (expressed as a decimal) from sunrise to sunset. This provides the total daily UVA exposure to a horizontal plane from the single solar noon-time OMI satellite UVA irradiance value for a range of possible cloud cover conditions that may be experienced over the 12-year study period.

UVA exposures of classroom and physical education teachers

The exposures to a horizontal plane were converted to exposures to the upper cheek employing a method that takes into account the ambient exposure to a horizontal plane, the activity of the subject, the ratio of the angle of the receiving plane compared to a horizontal plane and the protection factor provided by a hat (11, 12) as follows:

$$UVA_{Face} = UVA_{Day} \times AI \times GCF \times \frac{1}{PF} \qquad (6)$$

where UVA_{Face} is the total daily occupational UVA exposure to the cheek site, and UVA_{Day} is the total daily ambient UVA exposure evaluated from the noon-time satellite data (Equation 5). *AI* is the activity index, or the proportion of the daily UVA received in a working day based on the time outdoors. This has been previously reported for teachers at the location of the study site (27.5 ^{o}S, 152 ^{o}E) as 0.017 for physical education teachers and 0.003 for classroom teachers (13). The annual minimum and maximum solar noon SZA are 4.1^{o} and 51^{o} respectively and the minimum and maximum daylengths are 10.4 and 13.9 hours respectively. *PF* is the protection factor provided by a broad-brimmed hat to the cheek (11, 14). Previous research has measured the annual protection factor provided to the cheek by a broad-brimmed hat as 2, where this

number represents the ratio of the UVA received at the cheek site without hat protection to the expected UVA received with hat protection in place. Thus, *PF* for teachers not wearing a hat is 1. *GCF* is an anatomical Geometric Conversion Factor relating the incident UV received on a horizontal plane to a cylindrical upright approximation of the human body (15). The function of the solar zenith angle fitted to the data in Pope and Godar (15) and applied (16, 17) here is:

$$GCF = \frac{0.0001218\,SZA^2 - 10.99\,SZA + 1685}{SZA^2 - 166.5\,SZA + 8250} \qquad (7)$$

where *GCF* peaks at SZA=75º (0.62) (and is a minimum at SZA=0º (0.20). Thus, for an upright figure, the face is expected to receive the highest proportion of the available ambient when the sun is closer to the horizon, either approaching or following noon in the morning and afternoon, depending on the season.

For each day, the SZA applied according to Equation 7 was calculated using the average of the three SZA values at the three times of day (9:00, 11:00 and 13:30). These three times represent the time school teachers are expected to be outdoors and are based on previously determined activity indices (16).

The long-term facial UVA exposures over a 12-year period were calculated by summing the daily exposures to the school teachers from Equation (6). The weekend dates and the end of term dates for the Queensland School calendar year were not included in this summation. The assumption was that each of the classroom and the physical education teachers remained as either classroom or physical education teachers respectively over the period and no sunscreen was applied to the face.

RESULTS

Figure 3 shows the time series of the total daily occupational UVA exposures of the classroom teachers for the study site from 2005 to the end of 2016. This figure shows 1,940 total daily occupational UVA exposures depending on the school days when there were OMI satellite data available. Figure 3(a) represents the total daily UVA exposure to the cheek for the classroom teachers who were modelled wearing a broad-brimmed hat and not wearing a hat. The peaks and troughs in the four timeseries are due to the daily variation in cloud cover at the site that are superimposed on the seasonal variations in each year. For all four cases, the largest variations in the total daily UVA exposure are caused by the influence of cloud.

This figure shows a clear difference between the median of the total daily occupational UVA exposures likely to be received by the cheek for classroom teachers wearing a hat and not wearing a hat which were 0.53 and 1.06 kJ/m^2 for daily UVA exposures respectively. Figure 3(b) represents the total daily occupational UVA exposures to the cheek for the physical education teachers wearing a hat and not wearing a hat. The difference between the median of the total daily occupational exposure has a similar trend to Fig. 3(a) with medians of 2.99 and 5.98 kJ/m^2 for respective daily UVA exposures for the hat and no hat wearing cases. The differences in the UVA exposures to the cheek, for both the classroom teacher and physical education teacher for the hat and no hat wearing cases is a factor of two due to the broad-brimmed hat protection factor.

>Figure 3<

Figure 4 shows the graph of the total daily occupational cumulative UVA exposure from January 2005 to the end of 2016 to the cheek of the physical education teachers for the hat and no hat wearing cases. The graph shows the influence of not wearing a hat and increased outdoor activity on the increased cumulative exposures over a long period. The data showed that exposures for approximately six weeks at the end of each year were truncated due to the summer end of year school holiday period where there is no occupational exposure. This figure shows the differences in cumulative occupational UVA exposure received by the cheek between the four categories of teaching staff starting from a common point in January 2005. The influence of the cumulative exposure over the 12 years of the available data is evident where no hat wearing teachers have received a cumulative occupational UVA exposure to the cheek

at the end of the 12 years of 1,924 kJ/m^2 and 10,900 kJ/m^2 for the classroom and the physical education teachers respectively. Here, the physical education teachers receive an occupational exposure that was higher than a classroom teacher (who is expected to have a much lower outdoor activity index) by a factor of 5.7. In comparison, the hat wearing teachers received a cumulative occupational exposure at the end of the 12 years of 962 kJ/m^2 and 5,450 kJ/m^2 for the classroom and the physical education teachers respectively.

>Figure 4<

DISCUSSION

Previous research (6) has presented a technique to derive the daily erythemal exposure integral from the forecast maximum UV index by application of a Gaussian distribution function. In this research, it was shown that the Gaussian distribution is not as suitable for evaluating the daily UVA exposure. An alternative method was applied to evaluate the total daily UVA exposure to a horizontal plane to which a model was applied to derive the total daily UVA exposure to a working population group from single noon-time measurements of the OMI solar noon UVA irradiance. This research has calculated the total daily occupational UVA exposure to an anatomically effective facial site for classroom and physical education teachers. The assumption is that the teachers stay in the same teaching classification of either physical education teacher or classroom teacher over the 12 year period and that they maintain the same practice with regards to hat wearing. Compared to the ground-based measurements, the satellite derived daily total UVA exposures have a MAE of 10% for the sun not obscured data to 30% for the sun obscured data (9). The uncertainty in the occupational UVA exposures to the teachers is of this order of magnitude. Nevertheless, the results provide the means of calculating the cumulative influence on UVA exposure of different outdoor activities and hat wearing practices through UVA exposure monitoring on a time repetitive basis over an extended period.

Occupationally effective UVA exposures were calculated using the total daily UVA exposure derived for a horizontal plane from satellite data, the activity index of this occupational group, the relationship of the horizontal plane exposures to the vertical plane of a facial site, and the protection factor provided by a broad-brimmed hat.

Previous research has considered the erythemal UV to different occupational groups (18, 19, 20). However, it is also necessary to consider the occupational UVA exposure due to the associated health risks potentially associated with melanoma and photo aging (21). The UVA irradiance and the daily UVA exposure received by a horizontal plane from OMI data at a sub-tropical site have previously been evaluated (9, 10). This research has applied this previous methodology to provide the long-term UVA exposure to a working group of the population. This has been evaluated to the facial site of two groups of school teachers, both experiencing different periods of daily exposure outdoors. The face has been selected in this research as it is generally exposed when outdoors regardless of season, and the head and neck is a body site that experiences a high incidence of skin cancer.

There is a clear difference between the median of the total daily occupational UVA exposures to the cheek for the classroom teachers wearing a hat and not wearing a hat of 0.53 and 1.06 kJ/m^2 respectively. Similarly, the median of the daily exposures for the hat and no hat wearing physical education teachers were 2.99 and 5.98 kJ/m^2. Additionally, the plot of the total daily occupational cumulative UVA exposure over a period of 12 years has been shown for these two categories of teachers. Teachers can work longer than this, potentially 20 to 40 years and so the difference in UVA exposure between hat and no hat wearing teachers and classroom and physical education teachers will keep on accumulating. The cumulative difference in UVA exposure to the cheek due to the differences in outdoor activity and hat wearing practices were shown to be continually increasing over the 12 year study period for which OMI satellite noon time UVA irradiance data were available. These were for the 1,940 days when OMI satellite data were available. There were 14% of days occurring randomly when there were no OMI data available and these days were not taken into account in the cumulative exposures. Consequently, the cumulative UVA exposures may be underestimated by up to 14%.

The expected change in exposure increases linearly with year. After 12 years, the differences between the hat and no hat wearing cases is equivalent to an additional 962 and 5,450 kJ/m^2 of exposure for the classroom and physical education teachers respectively. This is clear evidence that UVA exposure to the face can be reduced through the regular use of a broad-brimmed hat. The use of a broad-brimmed hat is

essential during outdoor activities for the reduction of facial UVA exposure. Additionally, it is critically important to regularly apply broad-spectrum sunscreen to ensure protection is provided from the UVA waveband.

This research has employed UVA exposures from ground-based instrumentation to evaluate the scaling factor in equation (5). This can be extended to other sites where there are ground based measurements to enable the evaluation of the long-term cumulative UVA exposures to population groups. The methodology employed in this research has enabled evaluation of both the historical (from 2005 to 2016) and future UVA exposures to specific anatomical sites of both teaching and potentially other working population groups where surface instrumentation is not readily available.

Acknowledgements

The authors acknowledge the OMI mission scientists and associated NASA personnel for the production of the data used in this research effort.

REFERENCES

1. Kalliskota, S., J. Kaurola, P. Taalas, J.R. Herman, E.A. Celarier and N.A. Krotkov (2000) Comparison of daily UV doses estimated from Nimbus 7/TOMS measurements and ground-based spectroradiometric data. *J. Geophys. Res: Atmos*. **105**, D4 5059-5067. https://doi.org/10.1029/1999JD900926.
2. Soulen, P.F. and J.E. Frederick (1999) Estimating biologically active UV irradiance from satellite radiance measurements: A sensitivity study. *J. Geophys. Res: Atmos*. **104**, D4 4117-4126. https://doi.org/10.1029/1998JD200101
3. Paulescu, M., E. Paulescu, P. Gravila and V. Badescu (2012) Weather Modeling and Forecasting of PV Systems Operation. Springer Science & Business Media.
4. Bais, A.F., R.L. McKenzie, G. Bernhard, P.J. Aucamp, M. Ilyas, S. Madronich and K. Tourpali (2015) Ozone depletion and climate change: impacts on UV radiation. *Photochem. Photobiol. Sci*. **14**, 19-52. https://pubs.rsc.org/en/content/articlehtml/2015/pp/c4pp90032d.
5. Langston, M., L. Dennis, C. Lynch, D. Roe and H. Brown (2017) Temporal trends in satellite-derived erythemal UVB and implications for ambient sun exposure assessment. *Int. J. Env. Res. Public Health* **14**, 176. https://doi.org/10.3390/ijerph14020176.
6. Diffey, B (2009) A simple technique for estimating daily ambient erythemal ultraviolet from the ultraviolet index. *Photodermatol. Photoimmunol. Photomed*. **25**, 227-229. https://doi.org/10.1111/j.1600-0781.2009.00442.x
7. Diffey, B.L.S. (2002) Measurement of ultraviolet radiation. *Methods* **28**, 4-13. https://doi.org/10.1016/S1046-2023(02)00204-9.

8. Madronich, S., R. L. McKenzie, L.O. Björn and M.M. Caldwell (1998) Changes in biologically active ultraviolet radiation reaching the Earth's surface. *J. Photochem. Photobiol. B: Biol*. **46**, 5-19. https://doi.org/10.1016/S1011-1344(98)00182-1.
9. A Jebar, M A., A.V. Parisi, N.J. Downs and J. F. Turner (2020) Influence of clouds on OMI satellite total daily UVA exposure over a 12-year period at a southern hemisphere site. *Int. J. Remote Sensing* **41**, 272-283. https://doi.org/10.1080/01431161.2019.1641243.
10. A Jebar, M.A., A.V. Parisi, N.J. Downs and J.F. Turner (2018) Evaluated UVA irradiances over a twelve-year period at a subtropical site from ozone monitoring instrument data including the influence of cloud. *Photochem. Photobiol*. **94**, 1281-1288. https://doi.org/10.1111/php.12948.
11. Wong, J.C.F., D.K. Airey and R.A. Fleming (1996) Annual reduction of solar UV exposure to the facial area of outdoor workers in Southeast Queensland by wearing a hat. *Photodermatol. Photoimmunol. Photomed*. **12**, 131-135. https://doi.org/10.1111/j.1600-0781.1996.tb00189.x.
12. Diffey, B.L. (1992) Stratospheric ozone depletion and the risk of non-melanoma skin cancer in a British population. *Phys. Med. Biol*. **37**, 2267. https://iopscience.iop.org/article/10.1088/0031-9155/37/12/008.
13. Downs, N.J., S.L. Harrison, D.R.G. Chavez and A.V. Parisi (2016) Solar ultraviolet and the occupational radiant exposure of Queensland school teachers: a comparative study between teaching classifications and behavior patterns. *J. Photochem. Photobiol. B: Biol*. **158**, 105-112. https://doi.org/10.1016/j.jphotobiol.2016.02.018.

14. Gies, H.P., J. Javorniczky, C.R. Roy and S. Henderson (2006) Measurements of the UVR protection provided by hats used at school. *Photochem. Photobiol*. **82**, 750-754.

15. Pope, S.J. and D.E. Godar (2010) Solar UV geometric conversion factors: horizontal plane to cylinder model. *Photochem. Photobiol*. **86**, 457-466. https://doi.org/10.1111/j.1751-1097.2009.00679.x

16. Downs, N.J., T. Axelsen, P. Schouten, D.P. Igoe, A.V. Parisi and J. Vanos (2020) Biologically effective solar ultraviolet exposures and the potential skin cancer risk for individual gold medalists of the 2020 Tokyo Summer Olympic Games, *Temperature* **7**, 89-108, doi.org/10.1080/23328940.2019.1581427.

17. Igoe, D., A. Amar, P. Schouten, A.V. Parisi and J. Turner (2019) Assessment of biologically effective solar ultraviolet exposures for court staff and competitors during a major Australian tennis tournament. *Photochem. Photobiol*. **95**, 1461-1467.

18. Downs, N.J., A.V. Parisi and D. Igoe (2014) Measurements of occupational ultraviolet exposure and the implications of timetabled yard duty for school teachers in Queensland, Australia: preliminary results. *J. Photochem. Photobiol. B: Biol*. **131**, 84-89. https://doi.org/10.1016/j.jphotobiol.2014.01.012.

19. Vishvakarman, D. and J.C.F. Wong (2003) Description of the use of a risk estimation model to assess the increased risk of non-melanoma skin cancer among outdoor workers in Central Queensland, Australia. *Photodermatol. Photoimmunol. Photomed*. **19**, 81-88. https://doi.org/10.1034/j.1600-0781.2003.00012.x.

20. Vishvakarman, D., J.C.F. Wong and B.W. Boreham (2001) Annual occupational exposure to ultraviolet radiation in central Queensland. *Health Physics* **81**, 5, 536-544.

21. Battie, C., S. Jitsukawa, F. Bernerd, S.D. Bino, C. Marionnet and M. Verschoore (2014) New insights in photoaging, UVA induced damage and skin types. *Exp. Dermatol*. **23**, 7-12.

FIGURE CAPTIONS

Figure 1. The variation in (a) UVA and (b) erythemal UV five minute exposures recorded at one-hour intervals and measured for 186 cloud free days between October 2004 and December 2016. The data are divided by the largest value for each respective waveband with the different colours representing the different days.

Figure 2. Measured (a) UVA and (b) erythemal UV curves, normalized with respect to time of day and the peak value for each of the 186 cloud free days in the period October 2004 to December 2016 (points). All of the data falls within the thick black curves. Gaussian model approximations normalized to the peak of the measured data are plotted as dashed curves showing the range in possible Gaussian fits to the measured data.

Figure 3. Time series of the total daily occupational UVA exposures received at the cheek site of classroom teachers (AI = 0.003) and physical education teachers (AI = 0.017) for the cases of wearing a hat (PF = 2) and no hat (PF = 1).

Figure 4. The cumulative total daily occupational UVA exposure to the cheek expected for a teacher employed since January 2005. The four lines show the accumulation of the UVA exposures for classroom teachers (grey lines) and the physical education teachers (black lines), for the hat wearing cases with PF = 2 (dashed lines) and the no hat wearing cases with PF = 1 (solid lines).

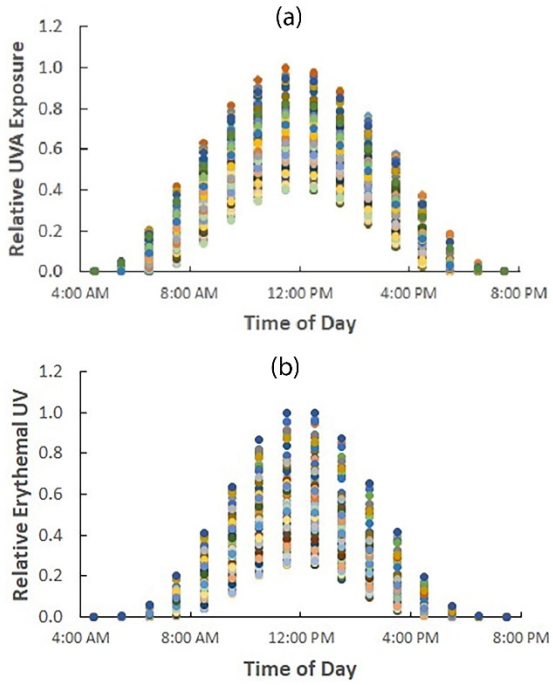
(a)
Relative UVA Exposure
1.2
1.0
0.8
0.6
0.4
0.2
0.0
4:00 AM
8:00 AM
12:00 PM
4:00 PM
8:00 PM
Time of Day
(b)
Relative Erythemal UV
1.2
1.0
0.8
0.6
0.4
0.2
0.0
4:00 AM
8:00 AM
12:00 PM
4:00 PM
8:00 PM
Time of Day

Figure 1

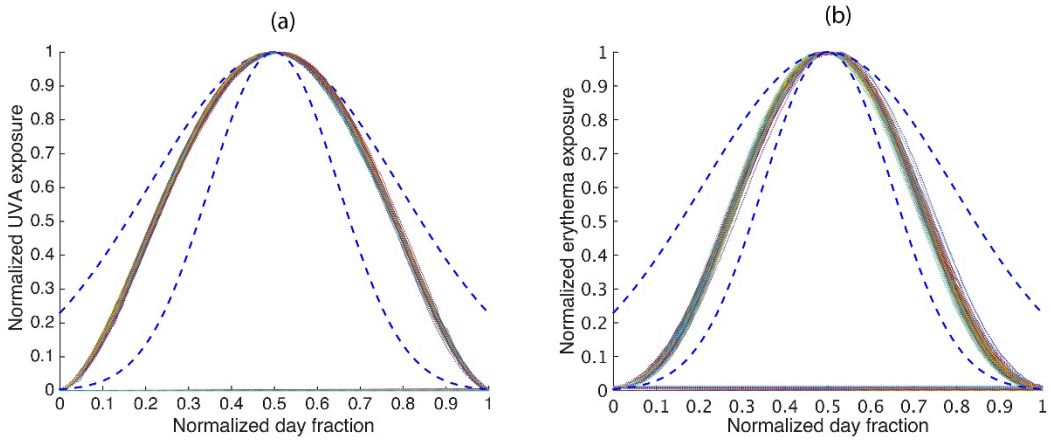
(a)
Normalized UVA exposure
Normalized day fraction
(b)
Normalized erythema exposure
Normalized day fraction

Figure 2

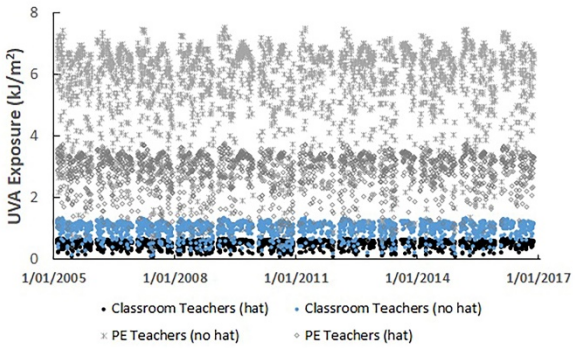
UVA Exposure (kJ/m²)
8
6
4
2
0
1/01/2005
1/01/2008
1/01/2011
1/01/2014
1/01/2017
Classroom Teachers (hat)
Classroom Teachers (no hat)
PE Teachers (no hat)
PE Teachers (hat)

Figure 3

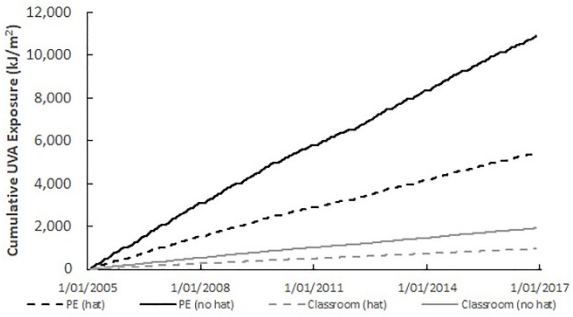
12,000
10,000
8,000
6,000
4,000
2,000
0
Cumulative UVA Exposure (kJ/m²)
1/01/2005
1/01/2008
1/01/2011
1/01/2014
1/01/2017
PE (hat)
PE (no hat)
Classroom (hat)
Classroom (no hat)

Figure 4